Echocardiography

Assessment of the Physiologic Significance of Coronary Disease With Dipyridamole Real-Time Myocardial Contrast Echocardiography

Comparison With Technetium-99m Sestamibi Single-Photon Emission Computed Tomography and Quantitative Coronary Angiography

Marcel Peltier, MD, David Vancraeynest, MD, Agnès Pasquet, MD, Taniyel Ay, MD, Véronique Roelants, MD, Anne-Marie D'hondt, MS, Jacques A. Melin, MD, PhD, Jean-Louis J. Vanoverschelde, MD, PhD

Brussels, Belgium

OBJECTIVES	The purposes of this study were to test whether quantitative real-time myocardial contrast echocardiography (RT-MCE) can detect coronary disease during pharmacologic stress and to compare this approach with single-photon emission computed tomography (SPECT).
BACKGROUND	Assessing myocardial perfusion during stress is important for the diagnosis and risk stratification of patients with coronary disease.
METHODS	Thirty-five patients referred for coronary angiography underwent RT-MCE and technetium-99m methoxyisobutylisonitrile (MIBI) SPECT at baseline and after 0.84 mg/kg dipyridamole. The modalities of RT-MCE and SPECT were analyzed both qualitatively and quantitatively. For this purpose, myocardial flow reserve was calculated from microbubble replenishment curves, and regional MIBI uptake was measured on circumferential profiles. Segments and vascular territories were categorized into five groups with increasing stenosis severity by quantitative coronary angiography.
RESULTS	With dipyridamole, beta and A × beta increased in all but the highest stenosis severity group. The increase in beta and A × beta was significantly lower in territories supplied by stenotic arteries than in those supplied by arteries with <50% stenosis. Graded decreases in beta and A × beta reserves were noted with increasing stenosis severity. Using the cutoff value of 2.00 for beta reserve, quantitative RT-MCE correctly identified 97% of the territories supplied by significant stenoses and 82% of those supplied by normal arteries. In contrast, quantitative SPECT correctly identified only 71% of the territories supplied by significant stenoses and 81% of those supplied by normal arteries.
CONCLUSIONS	This study shows that RT-MCE, with dipyridamole, can define the presence and severity of coronary disease in a manner that compares favorably with quantitative SPECT. (J Am Coll Cardiol 2004;43:257–64) © 2004 by the American College of Cardiology Foundation

Assessing myocardial perfusion and wall motion during stress is important for the diagnosis and risk stratification of patients with coronary artery disease (CAD) (1–6). Until recently, myocardial perfusion imaging required the use of radiolabeled flow tracers such as thallium-201 (1–3) and technetium-99m (^{99m}Tc)-sestamibi (4–6). Thanks to the development of new ultrasonic contrast agents and the introduction of electrocardiographically gated intermittent harmonic imaging, it has recently become possible to produce good-quality images of myocardial perfusion using conventional echocardiography, as well (7,8). Although intermittent imaging has clearly improved our ability to detect myocardial contrast and even to quantify myocardial blood flow (MBF), its clinical application in patients has been quite challenging, particularly during stress. It has recently been suggested that newer contrast imaging modalities, such as power-pulse inversion and power modulation, could obviate some of the problems encountered with intermittent imaging (9). These modalities indeed allow one to image myocardial contrast in real-time using low power emission. Coupled with short, high-power impulses that completely destroy the microbubbles within the field of view, they offer the unique opportunity to assess microbubble replenishment kinetics in real-time and hence MBF (10–12). In the present study, we therefore sought to evaluate the feasibility of measuring MBF with real-time contrast echocardiography (RT-MCE) in patients with

Abbreviations and Acronyms

CAD	=	coronary artery disease
LV	=	left ventricular
MBF	=	myocardial blood flow
MI	=	mechanical index
MIBI	=	methoxyisobutylisonitrile
QCA	=	quantitative coronary angiography
ROC	=	receiver-operating characteristics
RT-MCE	=	real-time myocardial contrast echocardiography
SPECT	=	single-photon emission computed tomography
^{99m}Tc	=	technetium-99m

known or suspected coronary disease and to compare the ability of dipyridamole RT-MCE and ^{99m}Tc methoxy-isobutylisonitrile (MIBI) single-photon emission computed tomography (SPECT) to detect angiographically significant coronary stenoses.

METHODS

Study population. The study population consisted of 35 consecutive patients (25 men; mean age 62 ± 10 years [range 44 to 81]) who were referred to our institution for diagnostic coronary angiography. All had normal resting global and regional left ventricular (LV) function. Patients with unstable angina, a previous myocardial infarction or coronary artery bypass graft surgery, severe arrhythmias, atrial fibrillation, second- or third-degree atrioventricular block, severe obstructive pulmonary disease, or insufficient image quality to allow adequate visualization of all myocardial segments from the apical windows were not considered for inclusion into the study. Each patient was informed of the investigative nature of the study, which had been approved by the Ethical Committee of our institution. All patients gave written, informed consent to participate in the study.

Selective coronary angiography and contrast left ventriculography were performed from the femoral approach after the echocardiographic and scintigraphic studies. Significant CAD was defined as >70% lumen diameter stenosis by quantitative coronary angiography (QCA) (Cardiovascular Angiographic Analysis system, Pie Medical Equipment, Maastricht, the Netherlands). Thirteen patients had single-vessel disease, 9 had multivessel disease, and 13 were free of any significant coronary stenosis. Overall, there were 10 left anterior descending (6 proximal, 2 mid, and 2 distal), 15 left circumflex (10 proximal and 5 mid), and 9 right (1 proximal, 6 middle, and 2 distal) coronary artery stenoses.

A ^{99m}Tc-MIBI SPECT study was obtained in every patient at rest and after dipyridamole-induced hyperemia. For this purpose, 30 mCi ^{99m}Tc-MIBI was injected intravenously. Approximately 1 to 2 h after injection, SPECT

images were obtained with a wide field-of-view rotating camera equipped with a high-resolution, parallel-hole collimator centered on the 140-keV photon peak with a 20% window (General Electric 400 AC/T, Milwaukee, Wisconsin). The camera was rotated over an arc of 180° in a circular orbit around the patient's thorax from a right anterior oblique angle of 40° to a left posterior angle of 40° at increments of 6° of 30 s each. The data were reconstructed in the same three long-axis views as echocardiography, with in-plane and *z*-axis resolutions of 13 mm, 6.2-mm per pixel sampling, and 6.2-mm separation between slices.

Myocardial contrast echocardiography. Perfluorocarbon-enhanced sonicated dextrose albumin (PESDA), a second-generation contrast agent consisting of decafluorobutane-filled albumin microbubbles with a mean diameter of 4.2 ± 0.5 μm and a mean concentration of 10^9/ml (as determined with a Coulter Multisizer Z2 Analyzer, Accucomp Software, Miami, Florida) was used in this study. A total dose 0.08 ml/kg PESDA was diluted in 100 ml of saline and administered intravenously using an infusion pump. The rate of infusion was carefully adjusted to maximize myocardial opacification while minimizing attenuation and blooming artifacts during real-time scanning. The mean infusion rate was 1.5 ± 0.3 ml/min.

Imaging was performed with a SONOS 5500 prototype system (Agilent Technologies, Andover, Massachusetts) equipped with a broadband S3 transducer (1 to 3 MHz). Color-coded power-modulation images were obtained from the apical windows using low-power (mechanical index [MI] between 0.1 and 0.2), real-time imaging at 20 frames/s. Power-modulation imaging is a pulse cancellation technique that transmits multiple pulses per image line, alternating full-amplitude pulses with half-amplitude pulses. Subtracting twice the return signal of the half-amplitude pulse from the return signal of the full-amplitude pulse cancels the linear response from the tissue, but not the nonlinear response from the bubbles. The dynamic range of the system is 20 dB, and the pulse repetition frequency is 2.5 kHz. Instrument settings were held constant throughout each experiment. To assess replenishment kinetics, profound microbubble destruction was produced by five consecutive high-power (MI of 1.7) frames transmitted on demand. Imaging then returned automatically to low-power, real-time scanning (MI between 0.1 and 0.2). Because microbubbles are destroyed by imaging at high MI, imaging at low MI reduces microbubble destruction and therefore allows microbubbles replenishment to be imaged in real-time.

Study protocol. Patients were studied at baseline and after dipyridamole infusion. After acquisition of the baseline gray-scale images from the three apical views, contrast infusion was started. The ultrasound system was then switched to low-power, real-time scanning. Once adequate cavity and myocardial opacification was achieved, RT-MCE data were recorded and digitized in a cine-loop format for

subsequent assessment of the replenishment kinetics. After acquisition of the baseline RT-MCE images, 0.84 mg/kg dipyridamole was infused over 6 min. Eight minutes after the start of the dipyridamole infusion, 30 mCi ^{99m}Tc-MIBI was injected intravenously. Immediately thereafter, RT-MCE was repeated.

Data analysis and image interpretation. The RT-MCE and SPECT data were analyzed both qualitatively and quantitatively using the American Society of Echocardiography's 16-segment model.

For both RT-MCE and SPECT, data were first analyzed visually by pairs of observers blinded to the clinical and other methods' results (Drs. Melin and Roelandts for SPECT; Drs. Peltier and Vancrayenest for MCE). Differences in opinion were resolved by consensus. With both methods, myocardial opacification and tracer uptake were judged as: 1 = normal; 0.5 = reduced (mild defect); 0 = absent (severe defect) (15). A reversible defect was defined as a visually discernible reduction in myocardial opacification or tracer uptake during stress that was no longer seen at rest. Because wall motion was normal at baseline, any resting defect was considered to be due to attenuation, and the segment was excluded from both the qualitative and quantitative analyses. Finally, if a defect was limited to a single basal segment of a vascular territory, this territory was still considered to be normal, and the defect was attributed to attenuation.

Quantitative analysis of RT-MCE sequences was performed on end-systolic images obtained in the apical four- and two-chamber views and in the apical long-axis view using the Freescan software package (Echotech, Hallbergmoos, Germany). For this purpose, three large, irregular, transmural regions of interest (ROI) encompassing the basal, mid-ventricular, and apical levels of the septum and lateral, anterior, and inferior walls, as well as the basal and mid-ventricular levels of the anteroseptal and posterior walls, were drawn on the last image of each dynamic power-modulation sequence (destruction flash, followed by a 15-s replenishment period). The myocardial ROIs were then copied onto all end-systolic power-modulation images and individually adjusted by hand to carefully avoid the right and LV cavities. The software package automatically calculates the mean video-intensity of each ROI and generates time-activity curves that were subsequently fitted to a monoexponential function: $y = A \cdot (1 - e^{-\beta t})$ (13), where beta represents the rate of rise in signal intensity, which reflects microbubble velocity, and A is the peak plateau amplitude, which reflects the microvascular cross-sectional area or myocardial blood volume (14). "A" was subsequently normalized for the blood pool video-intensity using the equation: normalized $A = 10^{([A - \text{blood pool}]/10)} \times 100$. Finally, the vasodilator reserve for beta and A × beta, an index of MBF, was calculated as the ratio of hyperemic to baseline values for these parameters.

Quantitative SPECT analysis was performed by use of circumferential profiles. For this purpose, an operator-defined ROI was drawn around the LV activity on each long-axis cross section. Myocardial activity was then calculated in six different sectors emanating from the center of the tomograms. Within each sector, the mean counts per pixel were computed for both the rest and stress images. Myocardial activity was further categorized as being ≤70% or >70% of the maximum activity. A normal response to dipyridamole was defined as >70% MIBI uptake at rest and during stress. A reversible defect was defined as MIBI uptake ≤70% during stress, which improved to >70% at rest. Finally, segments in which resting MIBI uptake was ≤70% were considered to be attenuation artifacts.

Statistical analysis. Continuous variables are expressed as the mean value ± SD. Comparisons between the different stenosis severity groups were performed using one-way analysis of variance (ANOVA), with the Bonferroni correction for post hoc comparisons. The relationship between the vasodilator reserve by RT-MCE and the severity of coronary stenoses by QCA was evaluated by least-squares fit regression analysis. Receiver-operating characteristics (ROC) curve analysis was used to identify the best cutoff values of vasodilator reserve for predicting the presence of significant coronary disease. Their predictive value was evaluated by computing the area under the ROC curves. The sensitivity, specificity, and accuracy of these cutoff values were evaluated on both vascular territory and patient bases. For this purpose, the septum, anteroseptal wall, and anterior wall were ascribed to the left anterior descending coronary artery, the lateral wall to the left circumflex coronary artery, and the inferior wall to the right coronary artery. Because of the varying vascular supply of the apex, this was allocated to any of the other involved territories. If the apex alone was involved, the left anterior descending coronary artery was imputed. Likewise, the posterior wall was ascribed to either the left circumflex or right coronary artery if either was involved. A p value <0.05 was considered as indicative of a statistically significant difference.

To determine intra- and interobserver variabilities, 10 sets of RT-MCE and SPECT images were reanalyzed separately by the observers who participated into the consensus reading. The interval between the initial analyses and those made for variability assessment was >3 months. Intra- and interobserver variabilities in quantitative RT-MCE and SPECT parameters were assessed by computing intraclass correlation coefficients using one-way ANOVA with a random factor and by calculating the limits of agreement between measurements made by use of Bland-Altman analysis. Kappa statistics were used to determine concordance between qualitative RT-MCE or SPECT parameters and QCA.

RESULTS

Patient characteristics are summarized in Table 1.
Myocardial contrast echocardiography. Of the possible 560 segments, 102 (19%) could not be adequately visualized
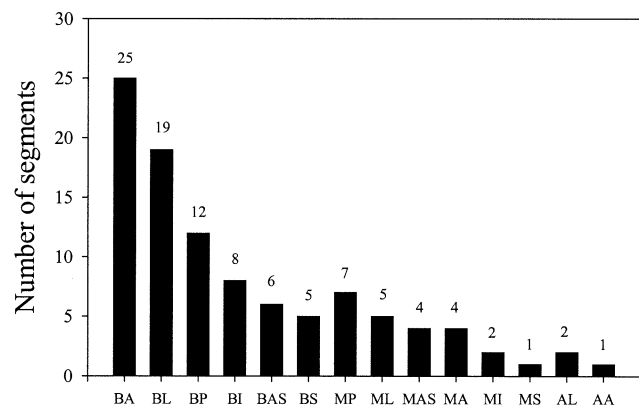
Table 1. Patient Characteristics

Demographic data	
Age (yrs)	62 ± 10
Gender (M/F)	25/10
Risk factors	
Hypertension	23 (66%)
Hypercholesterolemia	16 (45%)
Smoking	12 (34%)
Diabetes	6 (17%)
Previous PCI	7 (20%)
Pretest probability of CAD	52 ± 29%
Indications for coronary angiography	
Typical angina pectoris	13 (37%)
Atypical chest pain	17 (49%)
with a positive exercise ECG	10 (29%)
Preoperative risk assessment	5 (14%)

Data are presented as the mean value ± SD or number (%) of patients.
CAD = coronary artery disease; ECG = electrocardiogram; PCI = percutaneous coronary intervention.

at baseline and were therefore excluded from the analysis. Most of these segments (74%) were basal segments (Fig. 1). The remaining 458 segments (81%) were analyzed both qualitatively and quantitatively. Of these, 292 (64%) were supplied by arteries with <50% stenosis, 32 (7%) by arteries with 50% to 70% stenosis, 92 (20%) by arteries with 70% to 90% stenosis, and 42 (9%) by arteries with >90% stenosis. **Quantitative RT-MCE at baseline and during hyperemia.** With dipyridamole, the heart rate increased from 62 ± 10 to 84 ± 14 beats/min (p < 0.001). Systolic blood pressure decreased slightly from 151 ± 30 to 147 ± 25 mm Hg (p < 0.001). As a consequence, the rate-pressure product rose from 8,931 ± 2,549 to 12,246 ± 2,893 beats/min × mm Hg (p < 0.001).

The last refilling frame from the dipyridamole RT-MCE study (apical long-axis view) of a patient with >90% left circumflex coronary stenosis is illustrated in Figure 2. The corresponding SPECT image is also shown. Both
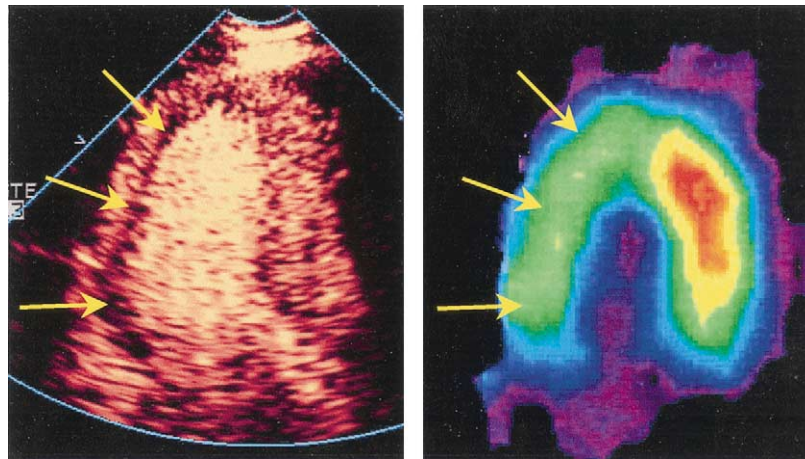
methods show the presence of a perfusion defect in the posterior wall. With RT-MCE, the defect is mostly subendocardial, whereas it appears transmural on SPECT. The time versus video-intensity curves obtained in the posterior and anteroseptal walls are shown in Figure 3. The microbubble velocity in the anteroseptal wall was faster than that in the posterior wall. The plateau video-intensity was also higher.

Table 2 shows the results of the quantitative RT-MCE analysis at baseline and during dipyridamole in the different stenosis severity groups. At baseline, no significant differences in A, beta, or A × beta were noted among the groups. With dipyridamole, beta and A × beta increased in all but the highest stenosis severity group. The increase in beta and A × beta was significantly lower in stenotic than in nonstenotic segments, however. Normalized A was not affected by dipyridamole, except in the highest severity group, in which it significantly decreased. Graded decreases in beta and A × beta reserves were noted with increasing coronary stenosis severity. A significant correlation was found between the percent lumen diameter stenosis derived from QCA and both beta (r = −0.85, p < 0.001) (Fig. 4) and A × beta (r = −0.81, p < 0.001) reserves by RT-MCE.

Diagnostic performance of MCE and SPECT. SEGMENT-BY-SEGMENT ANALYSIS. Empirical ROC curves were generated to determine the optimal cutoff values of beta reserve and A × beta reserve for prediction of significant coronary stenoses (Fig. 5). By use of a cutoff value of 2.00 for beta reserve, quantitative RT-MCE correctly identified 101 (75%) of 134 stenotic and 251 (77%) of 324 nonstenotic segments. Similarly, by use of a cutoff value of 1.96 for A × beta reserve, quantitative RT-MCE correctly identified 104 (78%) of 134 stenotic and 259 (80%) of 324 nonstenotic segments. Table 3 compares the diagnostic performance of quantitative and qualitative RT-MCE.

TERRITORY-BY-TERRITORY AND PATIENT-BY-PATIENT ANALYSES. The cutoff criteria derived from the segmental analysis were also used to assess the diagnostic performance of RT-MCE in individual vascular territories and in individual patients. Tables 4 and 5 compare the results of these analyses with those of qualitative MCE, qualitative SPECT, and quantitative SPECT.

OBSERVER VARIABILITY. The intraobserver variabilities in the measurements of beta reserve and A × beta reserve were 5.2% and 5.9%, respectively. The interobserver variabilities in the same parameters and in the quantitative SPECT measurements were 6.8%, 6.1%, and 7.9%, respectively. The intraobserver concordances for the visual analysis of MCE and SPECT images were 93% (kappa = 0.84) and 91% (kappa = 0.74), respectively. The interobserver concordances for the same parameters were 92% (kappa = 0.81) and 91% (kappa = 0.74), respectively.

Figure 1. Distribution of segmental artifacts on real-time myocardial contrast echocardiography. AL = anterior lateral; AA = apical anterior; BA = basal anterior; BAS = basal antero-septal; BI = basal inferior; BL = basal lateral; BP = basal posterior; BS = basal septal; MA = mid-anterior; MAS = mid antero-septal; ML = mid-lateral; MP = mid-posterior; MI = mid-inferior; MS = mid-septal.

Figure 2. Last refilling frame from the dipyridamole real-time myocardial contrast echocardiography study (apical long-axis view) of a patient with >90% left circumflex coronary stenosis **(left panel)** and the corresponding single-photon emission computed tomography image **(right panel)**.

DISCUSSION

This study demonstrates the feasibility of measuring MBF in patients with RT-MCE during dipyridamole stress and the accuracy of this method for detection of significant coronary disease. The results can be summarized as follows: 1) combined with the profound microbubble destruction produced by transient, high-power frames transmitted on demand, RT-MCE permits delineation of the time course of contrast reappearance in the myocardium in >80% of the segments. 2) The rate of contrast reappearance after microbubble destruction follows a monoexponential course, allowing the rate of rise in video-intensity (beta slope) and the peak myocardial intensity (plateau A) to be quantitated. 3) Beta and A × beta reserves, the ratio of hyperemic to baseline beta and A × beta, correlate inversely with the severity of the underlying coronary stenoses. 4) Reductions in beta and A × beta reserves below values of 2.00 and 1.96, respectively, allow significant CAD to be detected with both a high sensitivity and high specificity. 5) The diagnostic

performance of RT-MCE for detection of clinically significant coronary disease compares favorably with that of SPECT.

Rationale for use of RT-MCE. Regardless of the imaging technique or location of microbubble injection, myocardial contrast enhancement from microbubbles reflects myocardial blood volume (14). To gain information on MBF, a dedicated imaging strategy is needed, whereby the microbubbles are first destroyed by ultrasound, and their replenishment kinetics are then evaluated by progressively increasing the time between imaging pulses. Wei et al. (13) were the first to use this approach in open-chest animals. These authors demonstrated that the monoexponential increase in contrast intensity during intermittent imaging correlated closely with microsphere-derived MBF. Unfortunately, application of this approach to patients has been particularly challenging, mainly because of the complexity to the imaging strategy. Currently, the method requires 5 to 10
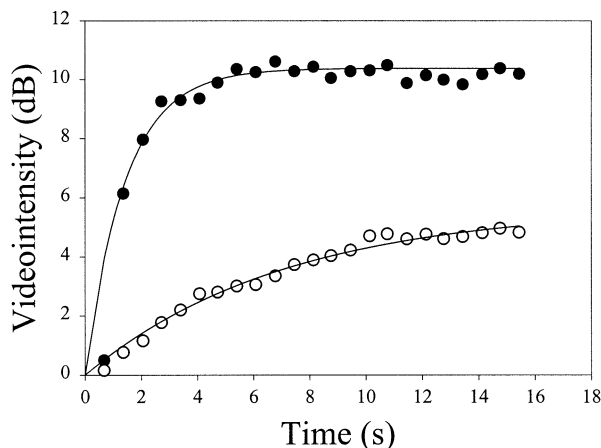
Figure 3. Time versus video-intensity curves obtained from the anteroseptal **(solid circles)** and posterior walls **(open circles)** of the patient whose images are shown in Figure 2. See text for details.

$$y = 2.65\,(1 - e^{0.09(x-100)})$$
$$r = 0.85$$
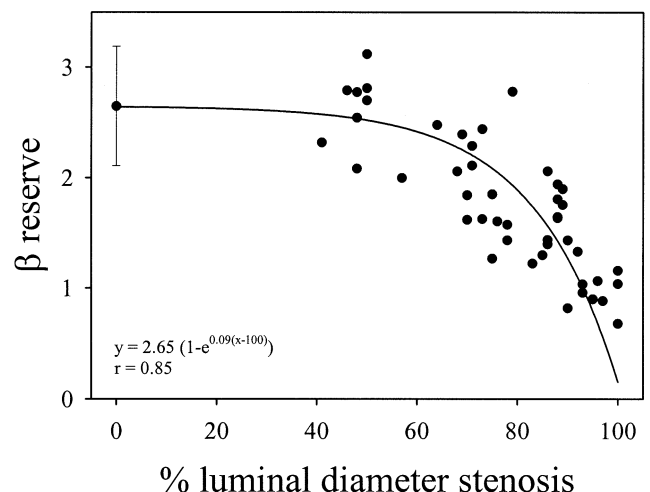
Figure 4. Scatterplots showing the relationship between percent lumen diameter stenosis by quantitative coronary angiography and beta reserve by myocardial contrast echocardiography in individual vascular territories.

Table 2. Myocardial Blood Flow and Myocardial Contrast Echocardiographic Data

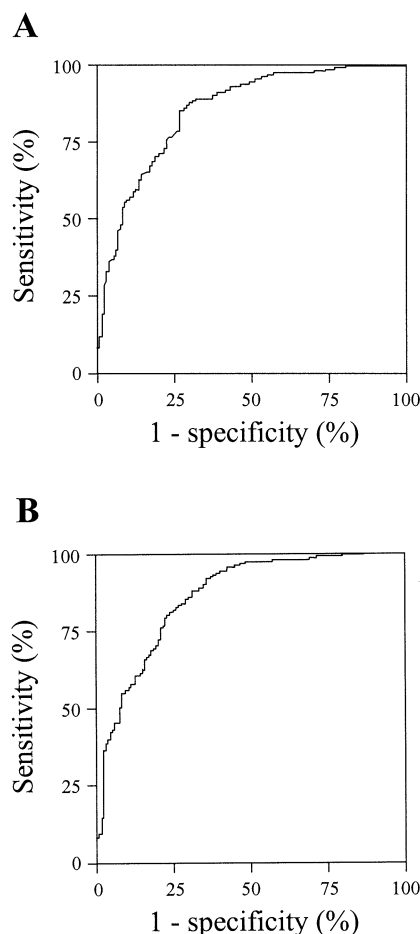|	Degree of Stenosis			
	<50%	**50%–70%**	**70%–90%**	**>90%**
Beta (s)				
Baseline	0.27 ± 0.07	0.28 ± 0.06	0.28 ± 0.07	0.28 ± 0.09
Dipyridamole	0.69 ± 0.21*	0.61 ± 0.18*	0.44 ± 0.20*†‡	0.30 ± 0.16†‡§
A (%LV)				
Baseline	10.1 ± 1.4	10.2 ± 1.7	10.3 ± 1.5	10.1 ± 1.5
Dipyridamole	10.1 ± 1.5	10.3 ± 0.2	9.8 ± 1.9	8.9 ± 1.4*†‡§
A × beta (dB/s)				
Baseline	2.7 ± 0.8	2.9 ± 1.0	2.9 ± 0.9	2.9 ± 1.2
Dipyridamole	7.0 ± 2.5*	6.3 ± 2.1*	4.4 ± 1.9*†‡	2.8 ± 1.9†‡§
Beta reserve	2.7 ± 0.9	2.3 ± 0.9	1.7 ± 0.7†‡	1.1 ± 0.6†‡§
A × beta reserve	2.7 ± 0.9	2.4 ± 0.9	1.6 ± 0.7†‡	1.0 ± 0.6‡§

*$p < 0.01$ vs. baseline. †$p < 0.01$ vs. <50%. ‡$p < 0.01$ vs. 50–70%. §$p < 0.01$ vs. 70–90%. Data are presented as the mean value ± SD.

A = peak plateau amplitude; beta = rate of rise in signal intensity; LV = left ventricle.

consecutive images to be obtained at different pulsing intervals (typically 300 ms and 1, 3, 5, and 8 s) during intermittent electrocardiography (ECG)-triggered imaging. As the refill kinetics need to be evaluated in the very same region in which the microbubbles have been destroyed, maintenance of a perfect alignment between the images is mandatory. At 8-s pulsing intervals, this becomes a real

Figure 5. Empirical receiver-operating characteristics curves generated for beta reserve (**A**) and A × beta reserve (**B**).

challenge. The RT-MCE approach allows one to circumvent this problem. By use of a pulse cancellation algorithm that eliminates the linear scatter from tissue, RT-MCE indeed permits imaging of microbubbles continuously at very low-power ultrasound, without destroying them. To assess replenishment kinetics, one simply needs to induce profound microbubble destruction by transmitting, on demand, a series of high-power frames and subsequently a return to low-power, real-time scanning. In a canine model, we (11) and others (10,12) have recently shown that microbubble refill parameters evaluated with RT-MCE correlated strongly with microsphere-derived MBF, over a wide range of flow conditions.

The present study demonstrates that assessment of MBF with RT-MCE is feasible in patients and results in an acceptable number of artifacts. Most importantly, these artifacts do not appear to limit the ability of RT-MCE to positively identify CAD. This is probably due to the fact that most of these artifacts (~75%) are confined to basal segments, whereas stress-induced perfusion defects mostly involve segments located near the apex. One of the advantages of RT-MCE is undoubtedly its ability to provide quantitative and hence more reproducible and less operator-dependent estimates of myocardial perfusion and perfusion reserve. Quite interestingly, these estimates strongly correlate with the severity of coronary stenoses determined by QCA, in a manner similar to that reported by Gould and Lipscomb (15). This strongly supports the use of this

Table 3. Diagnostic Performance of RT-MCE on a Segmental Basis

	RT-MCE		
	Qualitative MCE	**Beta Reserve 2.00**	**A × Beta Reserve 1.96**
Sensitivity	92/134 (69%)	101/134 (75%)	104/134 (78%)
Specificity	258/324 (80%)	251/324 (77%)	259/324 (80%)
Concordance	350/458 (76%)	352/458 (77%)	363/458 (79%)
	kappa = 0.46	kappa = 0.49	kappa = 0.53

RT-MCE = real-time myocardial contrast echocardiography; other abbreviations as in Table 2.

Table 4. Diagnostic Performance of RT-MCE and SPECT to Detect Significant Coronary Artery Disease in Individual Vascular Territories

| | RT-MCE | | | SPECT* | |
	Qualitative	Beta Reserve 2.00	A × Beta Reserve 1.96	Qualitative	Quantitative
Sensitivity	29/34 (85%)	33/34 (97%)	33/34 (97%)	25/34 (74%)	22/31 (71%)
Specificity	56/71 (79%)	58/71 (82%)	56/71 (79%)	57/71 (81%)	51/63 (81%)
Concordance	85/105 (81%)	91/105 (87%)	89/105 (85%)	82/105 (79%)	73/94 (78%)
	kappa = 0.60	kappa = 0.72	kappa = 0.68	kappa = 0.53	kappa = 0.51

*Quantitative single-photon emission computed tomography (SPECT) could not be obtained in 11 vascular territories for technical reasons.
RT-MCE = real-time myocardial contrast echocardiography; other abbreviations as in Table 2.

method, not only to detect the presence of CAD noninvasively but also to evaluate its physiologic significance once it has been angiographically identified. These results are in agreement with those previously reported by Wei et al. (22) with intermittent ECG-triggered B-mode harmonic imaging.

Relationship between perfusion by RT-MCE and SPECT. There are only a few studies comparing MCE and radionuclide imaging. The first multicenter trial on MCE showed that, under resting conditions, MCE had a poor correlation with SPECT (16). However, good correlations were observed when pharmacologic stress or exercise was used (17–21). This study is the first to compare the accuracy of both qualitative and quantitative RT-MCE and SPECT against QCA. Overall, our results are similar to those of previous investigations using intermittent imaging or qualitative RT-MCE. Our data nonetheless suggest that quantitative RT-MCE may offer some advantages over conventional qualitative assessments, as it is more reproducible and provides physiologic information on both MBF and myocardial blood volume.

Study limitations. Some specific aspects of the assessment of myocardial perfusion using power-modulation RT-MCE need to be critically appraised. First, the beta values in our study were generally lower than those reported by Wei et al. (13,22). There are two possible explanations for these differences. The first is the persistence of some degree of microbubble destruction during power-modulation RT-MCE, despite the use of low MI imaging. Indeed, switching from real-time to triggered intermittent imaging results

in a significant, albeit modest, increase in the degree of myocardial opacification (data not shown). The second relates to the induction of significant microbubble destruction within the LV cavity during the transmission of high-MI frames aimed at the destruction of microbubbles in myocardium. Calculated myocardial refilling rates may thus be contaminated by the simultaneous replenishment rate of the LV blood pool. Furthermore, quantitative assessment of replenishment kinetics requires knowledge of the contrast input function. Because of the limited dynamic range of the prototype system used, the input function could not be accurately measured, with contrast intensity in the blood pool often being close to 20 dB. We therefore made every effort to maintain constant delivery of contrast throughout the experiments. This probably explains why we did not observe any significant changes in plateau A in the nonstenotic segments during hyperemia, despite significant increases in the heart rate and rate-pressure product. Finally, the number of patients included in this study was relatively small. Accordingly, it has not been possible to establish whether quantitative RT-MCE was superior to qualitative assessment of MCE images or SPECT. Our data nonetheless suggest that quantitative RT-MCE is at least as accurate as SPECT for identifying significant CAD. However, our data need to be confirmed in larger studies before RT-MCE can be used routinely in daily clinical practice.

Conclusions. The present study indicates that RT-MCE with power modulation is feasible during dipyridamole stress in patients and that it can accurately identify significant CAD.

Table 5. Diagnostic Performance of RT-MCE and SPECT to Detect Significant Coronary Artery Disease in Individual Patients

| | RT-MCE | | | SPECT* | |
	Qualitative	Beta Reserve 2.00	A × Beta Reserve 1.96	Qualitative	Quantitative
Sensitivity	19/22 (86%)	22/22 (100%)	22/22 (100%)	18/22 (82%)	16/21 (76%)
Specificity	9/13 (69%)	10/13 (77%)	10/13 (77%)	11/13 (85%)	9/11 (82%)
Concordance	28/35 (80%)	32/35 (91%)	32/35 (91%)	29/35 (83%)	25/32 (78%)
	kappa = 0.69	kappa = 0.81	kappa = 0.81	kappa = 0.64	kappa = 0.54

*Quantitative single-photon emission computed tomography (SPECT) could not be obtained three patients for technical reasons.
Abbreviations as in Tables 2 and 4.

Reprint requests and correspondence: Dr. Jean-Louis J. Vanoverschelde, Division of Cardiology, Cliniques Universitaires St. Luc, Avenue Hippocrate, 10-2881, B-1200 Brussels, Belgium. E-mail: vanoverschelde@card.ucl.ac.be.

REFERENCES

1. Berger BC, Watson DD, Burwell LR, et al. Redistribution of thallium at rest in patients with stable and unstable angina and the effects of coronary artery bypass graft surgery. Circulation 1979;60:1114–25.
2. Gewirtz H, Beller GA, Strauss HW, et al. Transient defects of resting thallium scans in patients with coronary disease. Circulation 1979;59:707–13.
3. Glover DK, Ruiz M, Edwards NC, et al. Comparison between thallium-201 and ^{99m}Tc-sestamibi uptake during adenosine-induced vasodilation as a function of coronary stenosis severity. Circulation 1995;91:813–20.
4. Geleijnse ML, Fioretti PM. Selection of myocardial perfusion or function for the diagnosis of CAD. In: Marwick TH, editor. Cardiac Stress Testing and Imaging. New York, NY: Churchill Livingstone, 1996;97–111.
5. Faraggi M, Bok B, the Etude MIBI (EMIBI) Multicenter Study Group. Role of technetium-99m methoxyisobutylisonitrile single photon emission tomography in the evaluation of thrombolysis in acute myocardial infarction before and after admission to hospital. Eur J Nucl Med 1991;18:91–8.
6. DePuey EG, Garcia EV. Optimal specificity of thallium-201 SPECT through recognition of imaging artefacts. J Nucl Med 1989;30:441–9.
7. Porter TR, Xie F. Visually discernible myocardial echocardiographic contrast after intravenous injection of sonicated dextrose albumin microbubbles containing high molecular weight, less soluble gases. J Am Coll Cardiol 1995;25:509–15.
8. Porter TR, Li S, Kricsfeld D, Armbruster RW. Detection of myocardial perfusion in multiple echocardiographic windows with one intravenous injection of microbubbles using transient response second harmonic imaging. J Am Coll Cardiol 1997;29:791–9.
9. Vannan MA, Kuersten B. Imaging techniques for myocardial contrast echocardiography. Eur J Echocardiogr 2000;1:224–6.
10. Masugata H, Peters B, Lafitte S, Monet-Strachan G, Ohmori K, DeMaria AN. Quantitative assessment of myocardial perfusion during graded coronary stenosis by real-time myocardial contrast echo refilling curves. J Am Coll Cardiol 2001;37:262–9.
11. Van Camp G, Ay T, Pasquet A, et al. Quantification of myocardial blood flow and assessment of its transmural distribution with real-time power modulation myocardial contrast echocardiography. J Am Soc Echocardiogr 2003;16:263–70.
12. Leong-Poi H, Le E, Rim SJ, Sakuma T, Kaul S, Wei K. Quantification of myocardial perfusion and determination of coronary stenosis severity during hyperemia using real-time myocardial contrast echocardiography. Circulation 2001;14:1173–82.
13. Wei K, Jayaweera AR, Firoozan S, Linka A, Skyba DM, Kaul S. Quantification of myocardial blood flow with ultrasound-induced destruction of microbubbles administered as a constant infusion. Circulation 1998;97:473–83.
14. Kaul S, Jayaweera AR. Coronary and myocardial blood volumes: noninvasive tools to assess the coronary microcirculation. Circulation 1997;96:719–24.
15. Gould KL, Lipscomb K. Effects on coronary stenoses on coronary flow reserve and resistance. Am J Cardiol 1974;34:48–55.
16. Marwick TM, Brunken R, Meland N, et al. Accuracy and feasability of contrast echocardiography for detection of perfusion defects in routine practice: comparison with wall motion and MIBI-SPECT. J Am Coll Cardiol 1998;32:1260–9.
17. Kaul S, Senior R, Dittrich H, Raval U, Khattar R, Lahiri A. Detection of coronary artery disease with myocardial contrast echocardiography: comparison with ^{99m}Tc-sestamibi single photon computed emission tomography. Circulation 1997;96:785–92.
18. Porter TP, Li S, Kilzer K, Deligonul U. Correlation between quantitative angiographic lesion severity and myocardial contrast intensity during a continuous infusion of perfluorocarbon-containing microbubbles. J Am Soc Echocardiogr 1998;11:702–10.
19. Heinle SK, Noblin J, Goree-Best P, et al. Assessment of myocardial perfusion by harmonic power Doppler imaging at rest and during adenosine stress: comparison with ^{99m}Tc-sestamibi SPECT imaging. Circulation 2000;102:55–60.
20. Shimoni S, Zoghbi WA, Xie F, et al. Real-time assessment of myocardial perfusion and wall motion during bicycle and treadmill exercise echocardiography: comparison with single photon emission computed tomography. J Am Coll Cardiol 2001;37:741–7.
21. Porter TR, Xie F, Silver M, Kricsfeld D, O'Leary E. Real-time perfusion imaging with low mechanical index pulse inversion Doppler imaging. J Am Coll Cardiol 2001;37:748–53.
22. Wei K, Ragosta M, Thorpe J, Coggins M, Moos S, Kaul S. Noninvasive quantification of coronary blood flow reserve in humans using myocardial contrast echocardiography. Circulation 2001;103:2560–5.